

The study of $(\text{Ni,Mn,Co})\text{SO}_4$ as raw material for NMC precursor in lithium ion battery

Cite as: AIP Conference Proceedings **2708**, 070001 (2022); <https://doi.org/10.1063/5.0122596>
Published Online: 14 November 2022

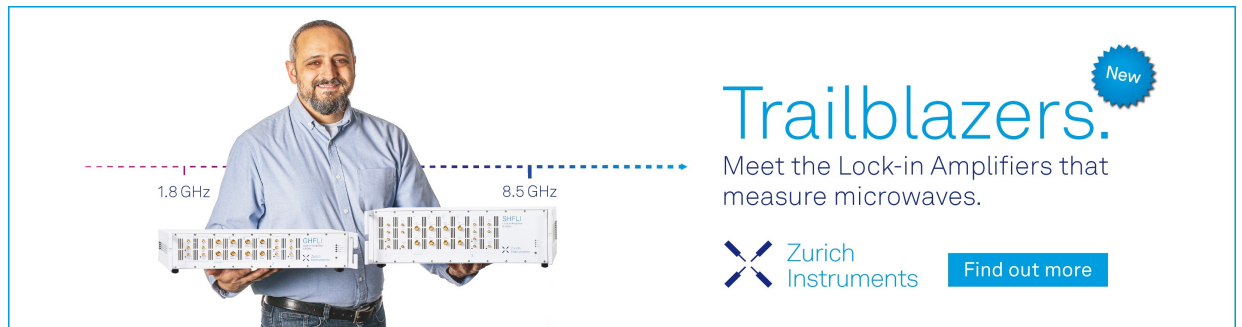
Evvy Kartini, Muhammad Fakhruddin, Widi Astuti, et al.



View Online



Export Citation



The advertisement features a man in a light blue shirt holding two Zurich Instruments lock-in amplifiers. A horizontal dashed line with arrows at both ends spans across the image, with a red dashed line segment on the left labeled '1.8 GHz' and a blue dashed line segment on the right labeled '8.5 GHz'. To the right of the man, the word 'Trailblazers.' is written in a large, blue, sans-serif font, with a small blue starburst containing the word 'New' above it. Below this, the text reads 'Meet the Lock-in Amplifiers that measure microwaves.' At the bottom right, the Zurich Instruments logo (a blue 'X' shape) is followed by the text 'Zurich Instruments' and a blue button with the text 'Find out more'.

The Study of (Ni,Mn,Co)SO₄ as Raw Material for NMC Precursor in Lithium Ion Battery

Evvy Kartini^{1, 2, a)}, Muhammad Fakhrudin^{1, 2}, Widi Astuti³, Slamet Sumardi³,
Mohammad Zaki Mubarak⁴

¹National Battery Research Institute, Edu Center Building Lt 2 Unit 22260 BSD City, South Tangerang 15331, Indonesia

²Nuclear Technology Organization- National Research Innovation Agency (BRIN), Indonesia, Puspiptek Bld.71, South Tangerang, Banten 15314

³Research Unit for Mineral Technology, National Research Innovation Agency (BRIN), Indonesia, Jl. Ir. Sutami, Serdang, Tj. Bintang District, South Lampung Regency, Lampung 35361

⁴Department of Metallurgical Engineering, Faculty of Mining and Petroleum Engineering, Institute Technology of Bandung, Jl. Ganesha, 10, Bandung 40132, Indonesia

^{a)} Corresponding author: evvy.kartini@gmail.com

Abstract. Recent technology of electric vehicle has been significantly improved due to the lithium-ion battery application that indispensable. Li(NMC)O₂ is one of the most highly demanding cathode materials. NMC cathode with high rich nickel exhibited excellent characteristic and high specific capacity. NMC active material is usually produced by calcination of NMC precursor mixed with lithium source. NMC precursor plays important role on determining quality of the active material NMC. The synthesis methods, such as co-precipitation are challenging to obtain the desire precursor, but the quality also depend on the raw materials. Those raw materials in powder form are NiSO₄, MnSO₄, CoSO₄ (metal sulphate). This paper describes the general properties of the NMC-sulphate, their crystal structure, microstructure and its elementary component by XRD, SEM and X-Ray Fluorescence (XRF). It is important to perform raw material characterizations before synthesizing into NMC Precursor. The XRD results showed the crystal structure of NiSO₄.6H₂O, MnSO₄.H₂O, CoSO₄.7H₂O corresponded to 100% phases Regersite, 100% Szmikite and 100% Moorhouseite, respectively. The XRF summary resulted that the nickel contents in NiSO₄.6H₂O was about 78% manganese content in MnSO₄.H₂O was about 77.7%, and cobalt content in CoSO₄.7H₂O was about 80.7%. The understanding properties of the raw materials was very important in order to achieve best quality of NMC precursor and the final product of NMC Cathode.

INTRODUCTION

The rapid progress of automotive battery market technology has been increasing since the invention of lithium-ion battery (LIB)[1]. The lithium-ion battery has an important role because of its price that will influence 40-45% of electric vehicle cost. Cathode materials such as NMC, NCA, LMO, and LFP have potential to become prominent battery chemistry due to their stable crystal structure, abundance resource, and relatively low cost [2]. It is predicted by 2025, the market share of NMC battery technology will increase from 26% to 41% because it has higher energy density than LFP and LMO as well as has better safety aspect than NCA [3][4]. Combination of nickel, manganese and cobalt in NMC cathode material attribute to the excellence performance. Since nickel delivers high energy density but poor stability, manganese owing to spinel structure that will impact to low internal resistance but has a low energy specific, cobalt exhibits structural stability but suffers from chemical stability [5][6].

There are several methods on preparing the precursor for active material NMC, such as co-precipitation, self-ignition combustion (SIC), molten salt, sol-gel, solid state, and hydrothermal [7][8][4]. NMC precursor that prepared by oxalate co-precipitation was done by dissolving all metal sulphates in form of $\text{NiSO}_4 \cdot 6\text{H}_2\text{O}$, $\text{MnSO}_4 \cdot \text{H}_2\text{O}$, $\text{CoSO}_4 \cdot 7\text{H}_2\text{O}$ in distilled water to get sulphate solution. Another oxalate solution was prepared as precipitating agent such as Oxalic Acid and NaOH. Then both solutions were mixed to become NMC precursor. Finally, those precursor NMC was added by lithium source that may come from $\text{Li}(\text{OH})$ or Li_2CO_3 then calcined at high temperature [9][10][11][12]. Although, there were many studies reported on the synthesizing the precursor and cathode of $\text{LiNi}_x\text{Mn}_y\text{Co}_z\text{O}_2$ (NMC), but only view paper explained about their raw materials as main components. Even if this very important, since determine not only the quality of the precursor, but also the end product of cathode NMC [6][13]. Therefore, in this paper, the metal (Ni, Mn, Co) sulphates, that used for making precursor will be investigated, in order to understand their properties and quality of the raw materials. The crystal structure and the components will be analysed by X-ray diffraction (XRD) and X-Ray Fluorescence (XRF), meanwhile the microstructure will be observed by using Scanning Electron Microscope (SEM).

METHODOLOGY

Materials

Technical grade $\text{NiSO}_4 \cdot 6\text{H}_2\text{O}$, $\text{MnSO}_4 \cdot \text{H}_2\text{O}$, $\text{CoSO}_4 \cdot 7\text{H}_2\text{O}$ were used as the source of transition metals of the cathode materials. Those samples are industrial grade which bought from Sumitomo Corporation.

Sample Characterization

A view gram of $\text{NiSO}_4 \cdot 6\text{H}_2\text{O}$, $\text{MnSO}_4 \cdot \text{H}_2\text{O}$, and $\text{CoSO}_4 \cdot 6\text{H}_2\text{O}$ were weighed. The crystal structure was conducted using an X-ray diffraction. A SEM was applied to observe the microstructure of the three samples. X-Ray Fluorescence (XRF) PANalytical Epsilon 3XLE was used to analyse elements content in the transition metal sulphates. The samples were put into the XRF holder, then placed into the XRF tool to get exposed from x-rays radiation. The results will be captured by detectors then will be displayed on the monitor.

RESULTS AND DISCUSSION

Nickel (II) sulphate ($\text{NiSO}_4 \cdot 6\text{H}_2\text{O}$)

Nickel(II) sulphate, or just nickel sulphate, usually refers to the inorganic compound with the formula $\text{NiSO}_4(\text{H}_2\text{O})_6$ as the hexahydrate nickel sulphate. This highly soluble blue green coloured salt is a common source of the Ni^{2+} ion for electroplating, while the anhydrous colour is light green (Figure 1).



FIGURE 1. Nickel Sulphate in form of anhydrous and hexahydrate, and its chemical structure

Figure 2 shows the x-ray diffraction of $\text{NiSO}_4 \cdot 6\text{H}_2\text{O}$. X-ray crystallography measurements show that $\text{NiSO}_4 \cdot 6\text{H}_2\text{O}$ corresponds to 100% regersite which consists of the octahedral $[\text{Ni}(\text{H}_2\text{O})_6]^{2+}$ ions. These ions in turn are hydrogen bonded to sulphate ions. Dissolution of the salt in water gives solutions containing the aquo complex $[\text{Ni}(\text{H}_2\text{O})_6]^{2+}$. All nickel sulphates are paramagnetic.

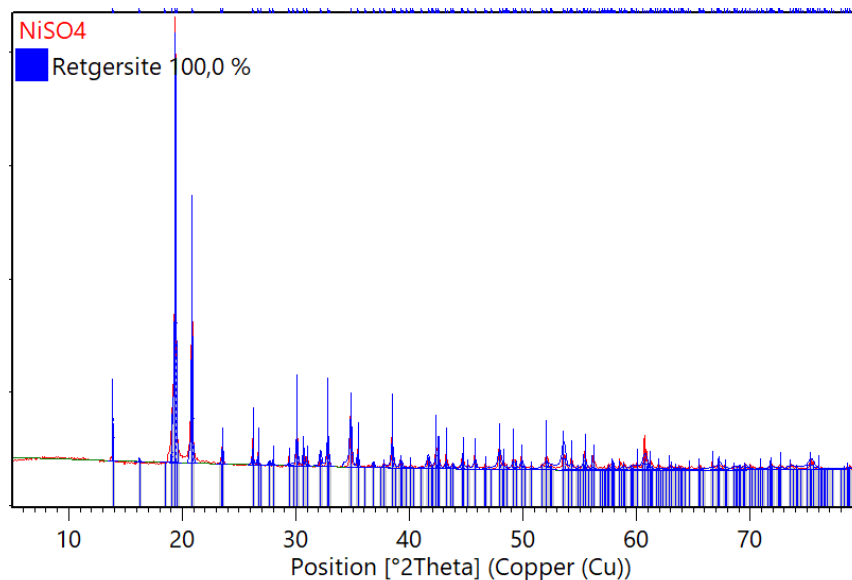


FIGURE 2. Refinement of Nickel Sulphate Hexahydrate $\text{NiSO}_4 \cdot 6\text{H}_2\text{O}$

Natural occurrence

Laterites, nickel ferrous limonite, and garnierite are the sources of nickel ore. Indonesia has the largest nickel resources in the world while laterite nickel ore is the most abundance resource in the world. Nickel processing technologies which widely adapted in the world are pyrometallurgy, hydrometallurgy, and combination of pyrometallurgy-hydrometallurgy. The pyrometallurgy process consist of reduction melting to produce ferro-nickel and reduction sulfurization melting to produce nickel-matte. On the other hand, hydrometallurgy method routes are ammonia leaching process and acid leaching process based on different leaching solutions. Combination methods of pyrometallurgy and hydrometallurgy are roasting-magnetic separation reduction and roasting-flotation reduction.

Nickel intermediate is the source of nickel sulphate production. The variety of nickel intermediates are nickel matte, Mixed Sulfide Precipitate (MSP), Mixed Hydroxide Precipitate (MHP), and briquette or powder of high purity nickel product. Nickel sulphate occurs as the rare mineral regersite, which is a hexahydrate. The second hexahydrate is known as nickel hexahydrate $(\text{Ni},\text{Mg},\text{Fe})\text{SO}_4 \cdot 6\text{H}_2\text{O}$. The heptahydrate, which is relatively unstable in air, occurs as morenosite. The monohydrate occurs as very rare mineral dwornikite $(\text{Ni},\text{Fe})\text{SO}_4 \cdot \text{H}_2\text{O}$.

Figure 3 shows the SEM image and crystalline salt of $\text{NiSO}_4 \cdot 6\text{H}_2\text{O}$. The image shows an agglomeration of unregular forms with some of them seems like ellipsoids. While its morphology in 5000 times magnification can be seen as follow with the diameter of particle is about 5 – 10 μm . The XRF analysis is listed in Table 1, showing the percentage of elements composed in $\text{NiSO}_4 \cdot 6\text{H}_2\text{O}$.

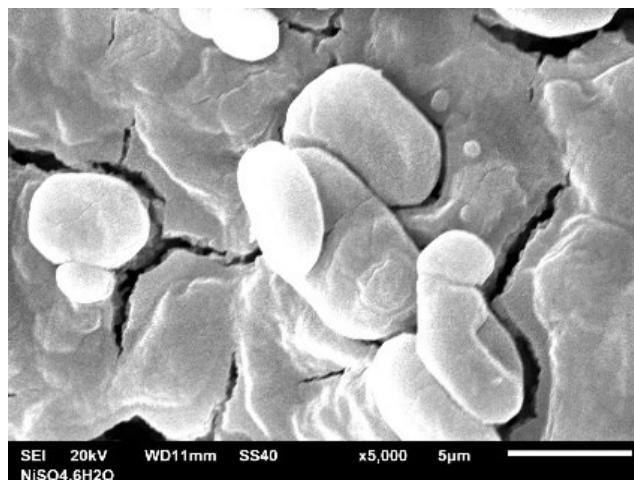


FIGURE 3. SEM image and crystalline salt of NiSO₄·6H₂O

The XRF revealed that the nickel, Ni and sulfur, S content from NiSO₄·6H₂O is about 78% and 21%, respectively. They are showing major contribution of elements in this blue crystal. However, there are some impurities appeared from the XRF data analysis, such as Al, Ca, Fe, Zr, Sn, Te and Dy with the total amounts of less than 1%. While the sulphur content is about twenty one percent. While the others are impurities like aluminium and iron that from literature are comes from the nickel-ore content which still can't be eliminated in extraction process. The calcium content which may come from the process of mixed hydroxide precipitate extraction. The others metal comes from overall leaching process and crystallization process of NiSO₄.

TABLE 1. XRF results on elements of NiSO₄·6H₂O

| Elements | Percentage |
|----------|------------|
| Al | 0.169% |
| S | 21.335% |
| Ca | 0.177% |
| Fe | 0.029% |
| Ni | 78.094% |
| Zr | 0.004% |
| Sn | 0.071% |
| Te | 0.020% |
| Dy | 0.100% |

Manganese(II) sulphate

Manganese(II) sulphate usually refers to the inorganic compound with the formula MnSO₄·H₂O. This pale pink deliquescent solid is a commercially significant manganese(II) salt as shown in Figure 4. Approximately 260,000 tonnes of manganese(II) sulphate were produced worldwide in 2005. It is the precursor to manganese metal and many other chemical compounds. Manganese-deficient soil is remediated with this salt.

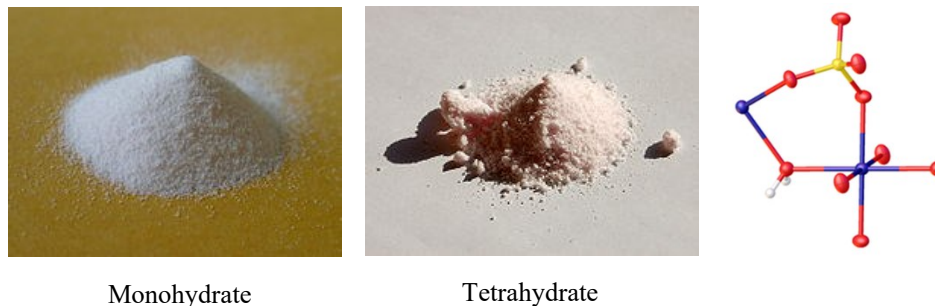


FIGURE 4. Manganese sulphate in different forms and its crystalline forms.

Structure

Like many metal sulphates, manganese sulphate forms a variety of hydrates: monohydrate, tetrahydrate, pentahydrate, and heptahydrate. Figure 4 shows various types of Mn-Sulphate monohydrate and tetrahydrate. All of these salts dissolve in water to give faintly pink solutions of the aquo complex $[\text{Mn}(\text{H}_2\text{O})_6]^{2+}$. Coordination sphere for Mn and S in the monohydrate. The O_6 coordination sphere is provided by four separate sulphate groups and a pair of mutually trans bridging aquo ligands.

Figure 5 shows the x-ray diffraction result of $\text{MnSO}_4 \cdot \text{H}_2\text{O}$. The refinement result shows that the crystal structure of $\text{MnSO}_4 \cdot \text{H}_2\text{O}$ related to 100% compound name Szmikite (chemical formula $\text{H}_2 \text{Mn}_1 \text{O}_5 \text{S}_1$, Mangan sulphate monohydrate, reference no.98-002-7099).

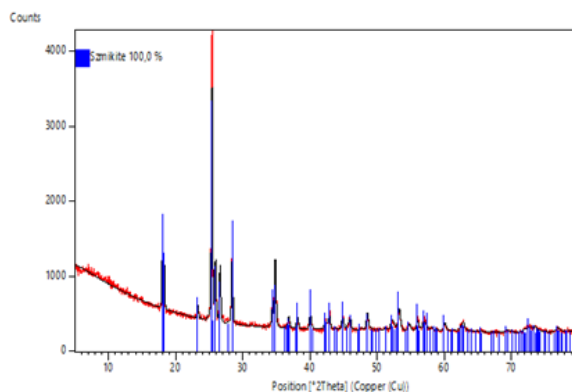


FIGURE 5. The x-ray diffraction of $\text{MnSO}_4 \cdot \text{H}_2\text{O}$

Figure 6 shows SEM image and crystalline powder of $\text{MnSO}_4 \cdot \text{H}_2\text{O}$. The shape forms are squares with the average sizes from 2-5 μm .

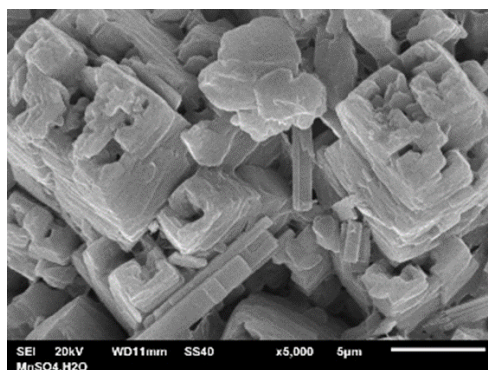


FIGURE 6. SEM image of the $\text{MnSO}_4 \cdot \text{H}_2\text{O}$

The manganese sulphate sample has almost the same percentage with the nickel content that previously described, namely 77.7% and the sulphur content is about 20.7%. The other content such as magnesium, aluminium, calcium carbonate, and nickel are the content from manganese ore that might come from the extraction process. Actually, the biggest impurity of manganese ore is iron meanwhile in this case, it is successful to separate iron from but it gives impact into the appearance of other impurities [14][15]. The size particles of MnSO_4 from SEM in Fig.6 were about $5\ \mu\text{m} - 10\ \mu\text{m}$ with the physical appearance is unregular rectangle shapes, made some layers. Table 2 shows the elements of $\text{MnSO}_4 \cdot \text{H}_2\text{O}$ from the XRF analysis [16]. The main component was 77.646% of Mn, followed by 20.645% S. The rest of elements consisted of Mg, Al, Ca, Sc, Co, Ni, Zn, Te, Pr, Er, Yb, Ta and Hg, with the total amount of impurities less than 2%. Based on Australian Government report, impurities content such as Na, Mg, Ca is need to be eliminated because they have negative impact on high-temperature morphology and cycling performance of lithium-ion battery [16].

TABLE 2. $\text{MnSO}_4 \cdot \text{H}_2\text{O}$

| Elements | Percentage |
|----------|------------|
| Mg | 0.192% |
| Al | 0.180% |
| S | 20.645% |
| Ca | 0.591% |
| Sc | 0.016% |
| Mn | 77.646% |
| Co | 0.151% |
| Ni | 0.132% |
| Zn | 0.216% |
| Te | 0.021% |
| Pr | 0.171% |
| Er | 0.027% |
| Yb | 0.003% |
| Ta | 0.003% |
| Hg | 0.005% |

Cobalt(II) Sulphate

Cobalt(II) sulphate (figure 7) is any of the inorganic compounds with the formula $\text{CoSO}_4(\text{H}_2\text{O})_x$. Usually cobalt sulphate refers to the hydrate $\text{CoSO}_4 \cdot 7\text{H}_2\text{O}$, which is one of the most commonly available salts of cobalt.

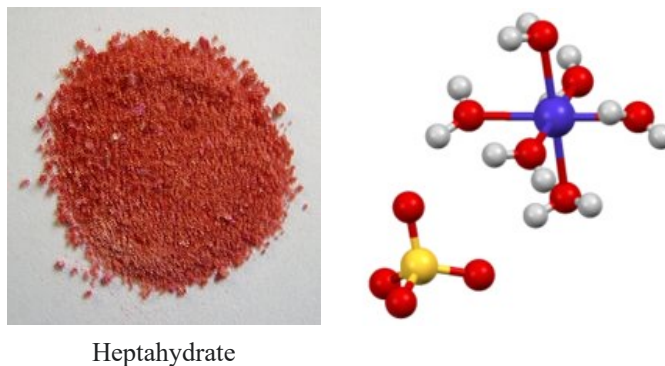


FIGURE 7. Cobalt sulphate heptahydrate (left) and structure of cobalt sulphate (right).

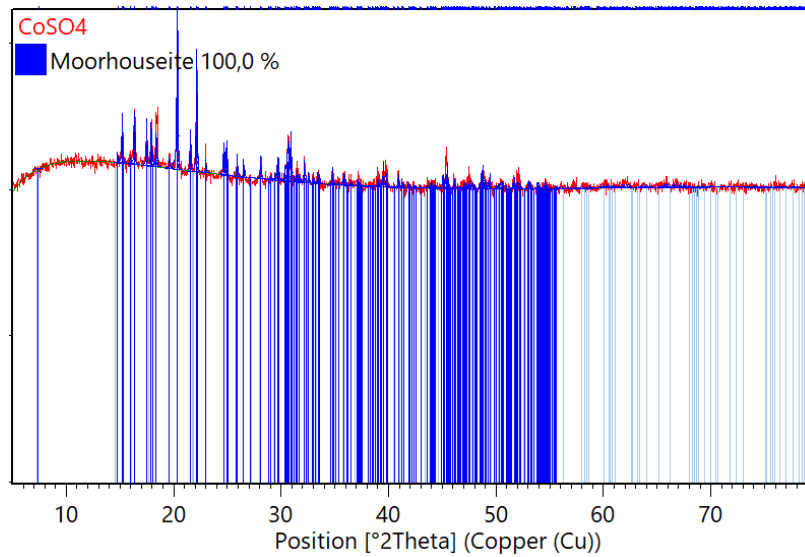


FIGURE 8. X-ray diffraction data of $\text{CoSO}_4 \cdot 7\text{H}_2\text{O}$

Figure 8 shows the x-ray diffraction pattern of $\text{CoSO}_4 \cdot 7\text{H}_2\text{O}$. the crystal structure of cobalt sulphate hexahydrate corresponds to 100% phase Moorhouseite. This is related to chemical formula $\text{H}_{12}\text{Co}_1\text{O}_{10}\text{S}_1$ and the space group $C 1 2/c 1$ [15].

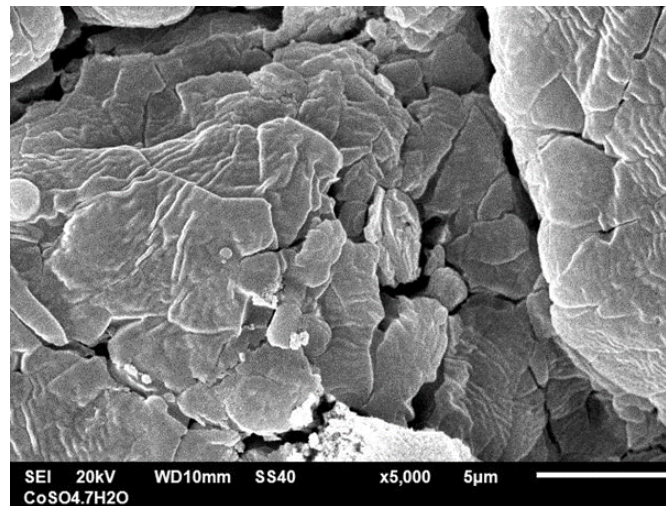


FIGURE 9. SEM image of morphology $\text{CoSO}_4 \cdot 7\text{H}_2\text{O}$

The XRF results are listed in Table 3 for $\text{CoSO}_4 \cdot 7\text{H}_2\text{O}$. The cobalt content in CoSO_4 is about 80.7% while the sulphur is about 18.8%. Cobalt and nickel usually come from the same ore, namely pyrolusite. This ore was extracted become mixed hydroxide precipitate (MHP) which contained cobalt and nickel. After that, MHP was separated by acid leaching process to get cobalt and nickel sulphate. Table 3 shows there is no nickel content on the CoSO_4 which means that the nickel can be well separated. The other elements are impurities that resulted from ore extraction and element separation. The SEM images showed that the particle of CoSO_4 was close each other and it was rather hard to distinguish the grain boundary. The morphology of cobalt sulphates formed like unregular flakes with the size ranging from 5-10 μm , as shown from the image of SEM in Figure 9.

TABLE 3. CoSO₄·7H₂O

| Elements | Percentage |
|----------|------------|
| Al | 0.104% |
| S | 18.796% |
| Ca | 0.154% |
| Co | 80.693% |
| Ga | 0.004% |
| Sn | 0.073% |
| Te | 0,016% |
| Eu | 0.152% |
| Ir | 0.007% |

CONCLUSION

The characteristic of the (Ni,Mn,Co)-Sulphates have been studied. The structure determined by x-ray diffraction identified the quality of the crystalline materials. The elements of metal sulphates were analyzed by XRF, showing not only the major components but also some of the impurities that were not detected via the x-ray diffraction data. The morphologies are different from each of the transition metals. The understanding of the insight of these raw materials were very important prior to the NMC precursor processing. In order to achieve the best properties of NMC active material cathode, there still needs a further step of sample purification in order to eliminate impurities. Since the concentration of impurities in precursor materials should be controlled due to maintain the chemical stability and performance in battery. Further characterization technique is suggested to be done using more advanced characterization technique (e.g. ICP-OES or ICP-MS).

ACKNOWLEDGMENTS

This work is partially supported by the National Battery Research Institute and the National Research Innovation Agency. Financial support from the National Priority Program through the BOPTN Bandung Institute of Technology in 2021 was really acknowledged.

REFERENCES

1. Z. Sun, L. Jiao, Y. Fan, F. Li, D. Wang, D. Han, L. Niu, Industrialization of tailoring spherical cathode material towards high-capacity, cycling-stable and superior low temperature performance for lithium-ion batteries, *RSC Adv.* 6 (2016) 97818–97824. <https://doi.org/10.1039/c6ra22040a>.
2. K. Chiba, A. Yoshizawa, Y. Isogai, Thermal safety diagram for lithium-ion battery using single-crystal and polycrystalline particles LiNi_{0.8}Co_{0.1}Mn_{0.1}O₂, *J. Energy Storage.* 32 (2020) 101775. <https://doi.org/10.1016/j.est.2020.101775>.
3. L. de Biasi, B. Schwarz, T. Brezesinski, P. Hartmann, J. Janek, H. Ehrenberg, Chemical, Structural, and Electronic Aspects of Formation and Degradation Behavior on Different Length Scales of Ni-Rich NCM and Li-Rich HE-NCM Cathode Materials in Li-Ion Batteries, *Adv. Mater.* 31 (2019). <https://doi.org/10.1002/adma.201900985>.
4. H.J. Noh, S. Youn, C.S. Yoon, Y.K. Sun, Comparison of the structural and electrochemical properties of layered Li[NixCoyMnz]O₂ (x = 1/3, 0.5, 0.6, 0.7, 0.8 and 0.85) cathode material for lithium-ion batteries, *J. Power Sources.* 233 (2013) 121–130. <https://doi.org/10.1016/j.jpowsour.2013.01.063>.
5. C. Julien, A. Mauger, K. Zaghib, H. Groult, Optimization of layered cathode materials for lithium-ion batteries, *Materials (Basel).* 9 (2016). <https://doi.org/10.3390/MA9070595>.
6. Y. Zhang, H. Cao, J. Zhang, B. Xia, Synthesis of LiNi_{0.6}Co_{0.2}Mn_{0.2}O₂ cathode material by a carbonate co-precipitation method and its electrochemical characterization, *Solid State Ionics.* 177 (2006) 3303–3307. <https://doi.org/10.1016/j.ssi.2006.09.008>.
7. J. Li, J. Camardese, S. Glazier, J.R. Dahn, Structural and electrochemical study of the Li-Mn-Ni oxide

- system within the layered single phase region, *Chem. Mater.* 26 (2014) 7059–7066. <https://doi.org/10.1021/cm503505b>.
8. H. Li, J. Li, X. Ma, J.R. Dahn, Synthesis of Single Crystal LiNi_{0.6}Mn_{0.2}Co_{0.2}O₂ with Enhanced Electrochemical Performance for Lithium Ion Batteries, *J. Electrochem. Soc.* 165 (2018) A1038–A1045. <https://doi.org/10.1149/2.0951805jes>.
 9. C. Liang, F. Kong, R.C. Longo, K.C. Santosh, J.S. Kim, S.H. Jeon, S.A. Choi, K. Cho, Unraveling the Origin of Instability in Ni-Rich LiNi_{1-2x}CoxMnxO₂ (NCM) Cathode Materials, *J. Phys. Chem. C.* 120 (2016) 6383–6393. <https://doi.org/10.1021/acs.jpcc.6b00369>.
 10. C.M. Julien, A. Mauger, NCA, NCM811, and the Route to Ni-Richer Lithium-Ion Batteries, *Energies.* 13 (2020) 6363. <https://doi.org/10.3390/en13236363>.
 11. J. Zheng, P. Yan, L. Estevez, C. Wang, J.G. Zhang, Effect of calcination temperature on the electrochemical properties of nickel-rich LiNi_{0.76}Mn_{0.14}Co_{0.10}O₂ cathodes for lithium-ion batteries, *Nano Energy.* 49 (2018) 538–548. <https://doi.org/10.1016/j.nanoen.2018.04.077>.
 12. A. Chakraborty, S. Kunnikuruvan, S. Kumar, B. Markovsky, D. Aurbach, M. Dixit, D.T. Major, Layered Cathode Materials for Lithium-Ion Batteries: Review of Computational Studies on LiNi_{1-x-y}CoxMnyO₂ and LiNi_{1-x-y}CoxAlyO₂, *Chem. Mater.* 32 (2020) 915–952. <https://doi.org/10.1021/acs.chemmater.9b04066>.
 13. S. Dou, Review and prospect of layered lithium nickel manganese oxide as cathode materials for Li-ion batteries, *J. Solid State Electrochem.* 17 (2013) 911–926. <https://doi.org/10.1007/s10008-012-1977-z>.
 14. J. Xiao, W. Ding, Y. Peng, T. Chen, K. Zou, Z. Wang, Extraction of nickel from garnierite laterite ore using roasting and magnetic separation with calcium chloride and iron concentrate, *Minerals.* 10 (2020) 1–13. <https://doi.org/10.3390/min10040352>.
 15. L. Perring, M. Nicolas, D. Andrey, C. Fragnière Rime, J. Richoz-Payot, S. Dubascoux, E. Poitevin, Development and Validation of an ED-XRF Method for the Fast Quantification of Mineral Elements in Dry Pet Food Samples, *Food Anal. Methods.* 10 (2017) 1469–1478. <https://doi.org/10.1007/s12161-016-0695-z>.
 16. Future Battery Industries CRC, Li-ion battery cathode manufacture in Australia, Dep. Ind. Innov. Sci. Aust. Government. (2020). <https://fbicrc.com.au/wp-content/uploads/2020/07/>.